Electronic Supplementary Material (ESI) for Soft Matter.

Supporting Information for

Molecular-level insights into tripolyphosphate and pyrophosphate templated membrane assembly

Mahesh Prasad, Bibhas Hazra, Avijit Sardar, Raki Mandal, Soumajit Gayen, and Pradip K. Tarafdar*

Dry-down reactions

The dry-down reactions have been proposed as one of the important primitive earth reactions to synthesize short peptides, depsipeptides, *N*-acyl amino acids etc. We performed dry-down reactions with aqueous solutions of fatty acids (lauric acid, myristic acid, and palmitic acid) and choline (1:1 mixture, 20 mM each) in pH 3.0 buffer at 90 ºC. After two wet-dry cycles over a period of 24 hours, we checked the mass spectrum of the reaction mixture. Control reactions with either fatty acids or choline were performed. We detected a mass peak at 286.276 from the lauric acid-choline mixture, which corresponds to the *O*-lauroylcholine (OLC) in the solution (Figure S1). This observation indicated that dry-down reaction might be a plausible pathway for the synthesis of *O*-acylcholines during early evolution.

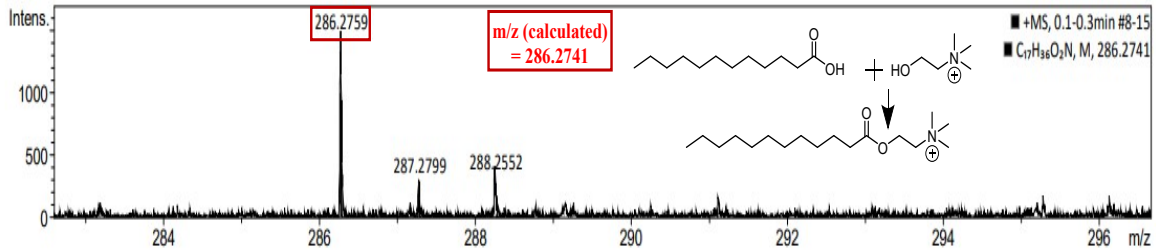

Figure S1: Detection of OLC from dry-down reactions with lauric acid and choline.

General procedure for the formation of ester bond (GP1)

Free carboxylic acid (lauric acid/ myristic acid/ palmitic acid) containing compound (1 eq.) was dissolved in 20 mL of dry DCM in an ice water bath. Dicyclohexylcarbodiimide (DCC) (1.2 eq.) and DMAP (0.2 eq.) were added to the reaction mixture followed by the *N*, *N*-Dimethyl ethanolamine (2-Dimethylaminoethanol) (1.2 eq.). The reaction mixture was stirred for 20 hrs at room temperature under nitrogen atmosphere. After completion, first DCM was evaporated, cold ethyl acetate (around 50 mL) was added to the residue and dicyclohexyl urea (DCU) was filtered off. The filtrate was evaporated in a rotary evaporator under reduced pressure to yield the desired compound (A). The product was purified in silica gel (60-120 or 100-200 mesh) using *n* hexane-ethyl acetate as eluent.

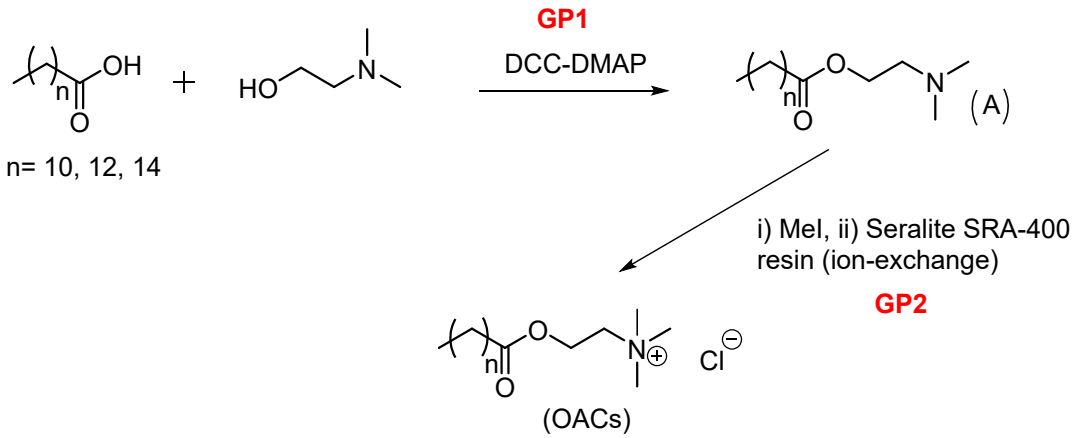

Scheme S1: Chemical synthesis of OACs.

General procedure for the formation of OACs (GP2)

Next, product (A) (1.0 eq.) was reacted with methyl iodide (1.2 eq.) in 10 ml of dry DCM solvent in an ice bath. After 2 hours white precipitate was floating in the reaction mixture. Finally, this white precipitate was filtered out and passed through Seralite SRA-400 ion exchange resin. The solvent was removed to get the final product (OLC/ OMC/ OPC). The product was characterized by NMR spectroscopy and high-resolution mass spectrometry.

Procedure for chemical synthesis of OLC

OLC was synthesized by following GP1 (Yield: 758 mg, 70%), and GP2 (Yield: 431 mg, 48%) **(Scheme S1)**. ^{1}H NMR (500 MHz, DMSO) δ 4.46-4.42 (m, 2H), 3.68 – 3.62 (m, 2H), 3.12 (s, 9H), 2.34 (t, J = 7.4 Hz, 2H), 1.58 – 1.50 (m, 2H), 1.31-1.20 (m, 16H), 0.86 (t, J = 6.7 Hz, 3H). HRMS: m/z 286.2768 $[M]^{+}$; M_{calcd}: 286.2741.

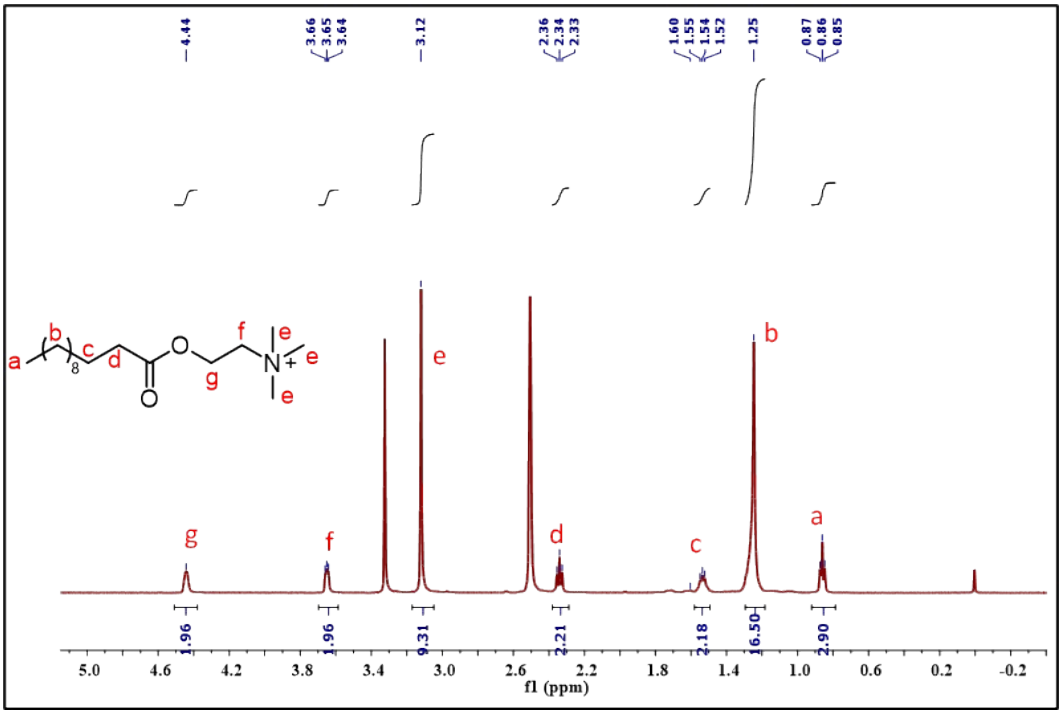

Figure S2: ^{1}H-NMR of OLC.

^{13}C NMR (126 MHz, DMSO) δ 172.81, 64.23, 58.13, 53.42, 33.82, 31.75, 29.46, 29.35, 29.17, 29.17, 28.90, 24.92, 24.66, 22.55, 14.42.

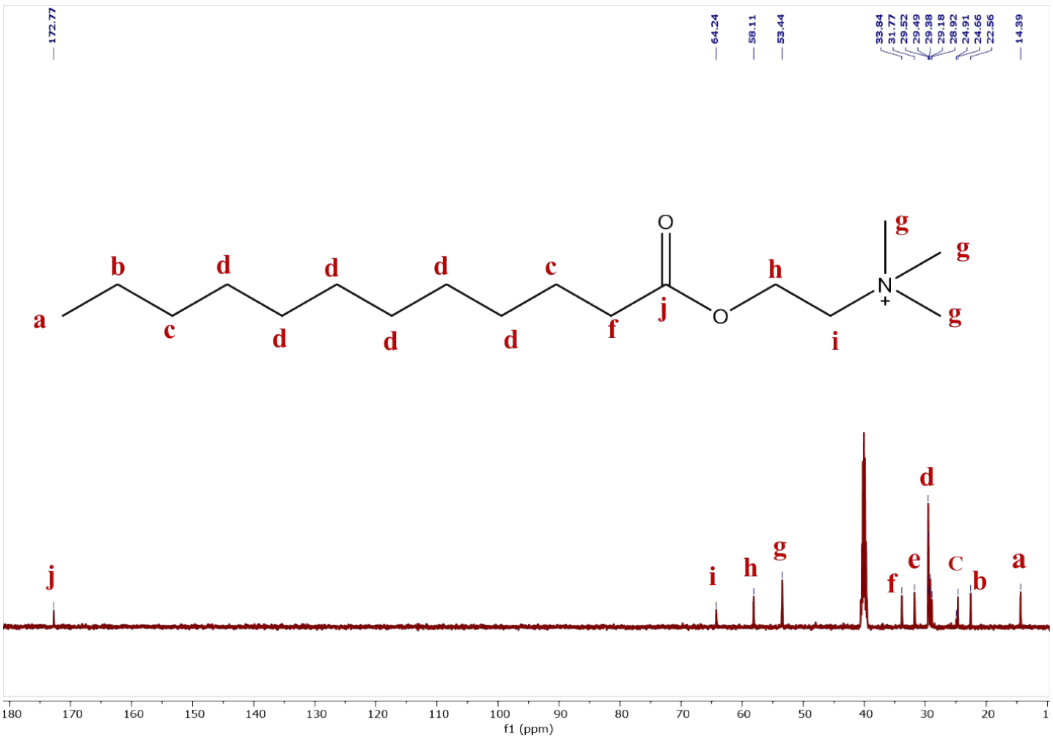

Figure S3: ^{13}C-NMR of OLC.

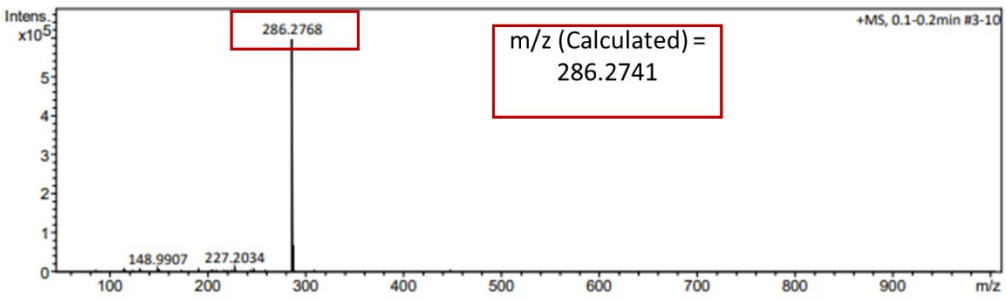

Figure S4: HRMS of chemically synthesized OLC.

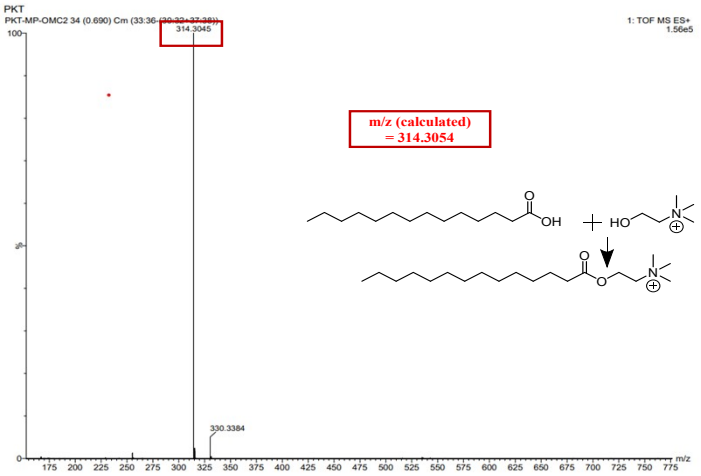

Figure S5: Detection of OMC from dry-down reactions with myristic acid and choline.

Procedure for chemical synthesis of OMC

OMC was synthesized by following GP1 (Yield: 1010 mg, 80%), and GP2 (Yield: 708mg, 60%) **(Scheme S1)**. ^{1}H NMR (500 MHz, DMSO) δ 4.46 – 4.42 (m, 2H), 3.66 – 3.60 (m, 2H), 3.11 (s, 9H), 2.35-2.30 (t, J = 7.4 Hz, 2H), 1.57-1.48 (m, 2H), 1.27-1.20 (m, 20H), 0.86 (t, J = 6.7 Hz, 3H). HRMS: m/z 314.3102 $[M]^{+}$; M_{calcd}: 314.3050.

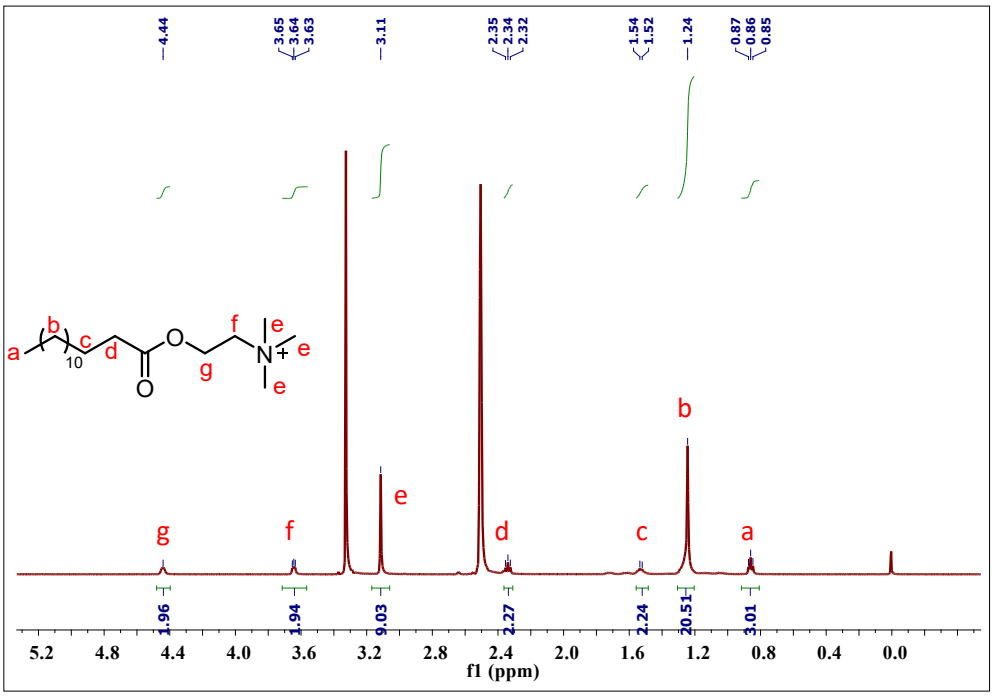

Figure S6: ^{1}H-NMR of OMC.

^{13}C NMR (126 MHz, DMSO) δ 173.26, 64.51, 58.11, 53.75, 33.85, 31.79, 29.51, 29.49, 29.49, 29.47,29.45, 29.35, 29.18, 28.91, 24.66, 22.60, 14.47.

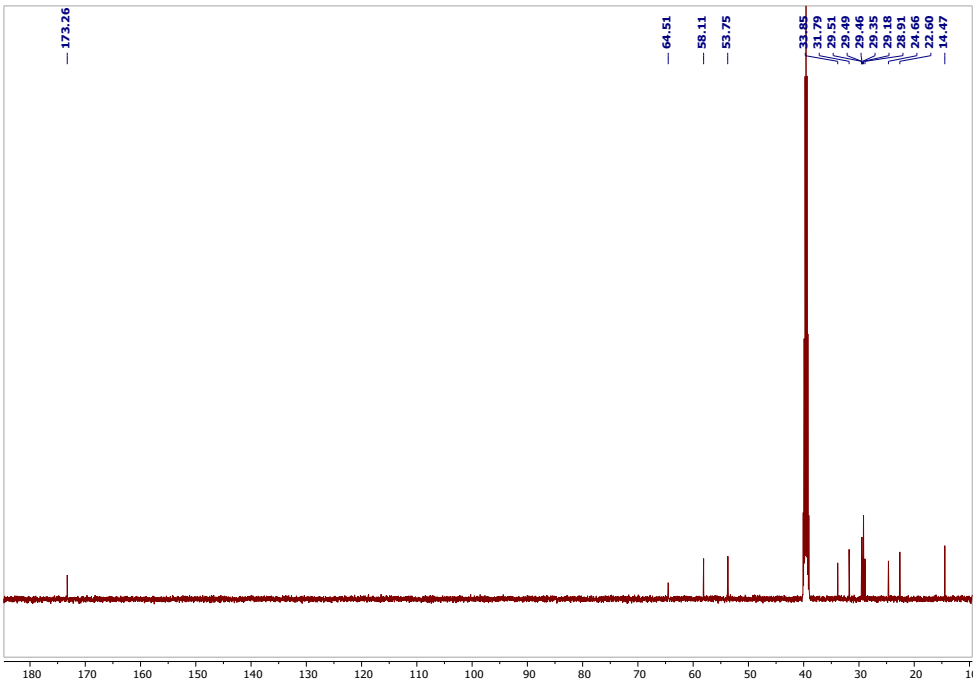

Figure S7: ^{13}C-NMR of OMC.

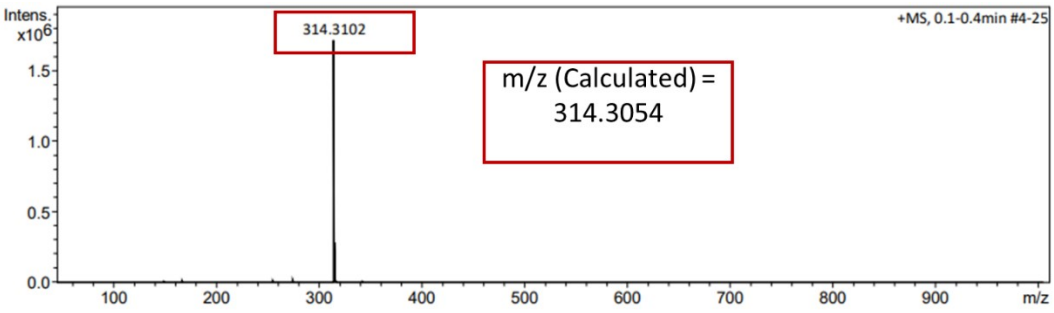

Figure S8: HRMS of chemically synthesized OMC.

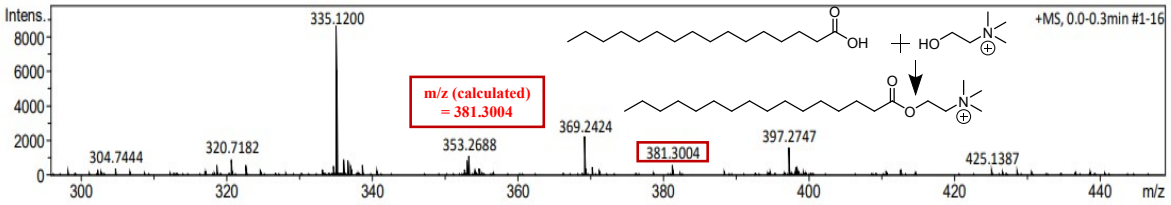

Figure S9: Detection of OPC from dry-down reactions with palmitic acid and choline.

Procedure for chemical synthesis of OPC

OPC was synthesized by following GP1 (Yield: 600 mg, 84 %), and GP2 (Yield: 463 mg, 67 %) **(Scheme S1)**. ^{1}H-NMR (500 MHz, DMSO) δ 4.46-4.42 (m, 2H), 3.68 – 3.60 (m, 2H), 3.12 (s, 9H), 2.34 (t, J = 7.4 Hz, 2H), 1.60 – 1.49 (m, 2H), 1.30-1.20 (m, 24H), 0.86 (t, J = 6.7 Hz, 3H). HRMS: m/z 342.3407 $[M]^{+}$; M_{calcd}: 342.3367.

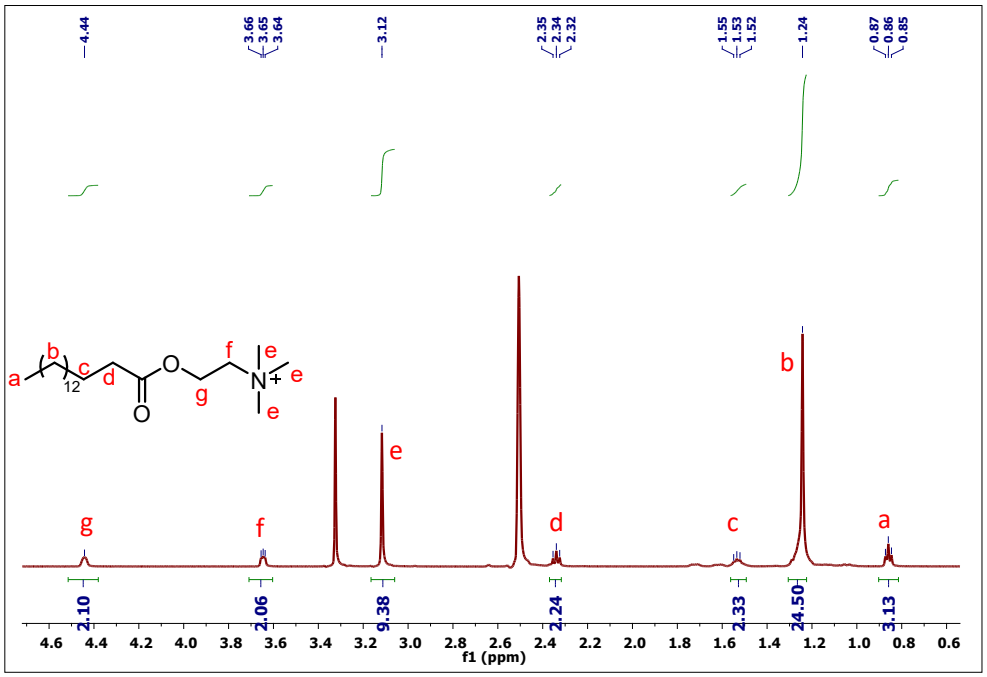

Figure S10: ^{1}H-NMR of OPC

^{13}C NMR (126 MHz, $CDCl_3$) δ 172.94, 65.41, 57.85, 55.00, 34.26, 34.04, 32.03, 29.80, 29.77, 29.74, 29.61, 29.47, 29.40, 29.25, 25.73, 25.07, 24.80, 22.80, 14.23.

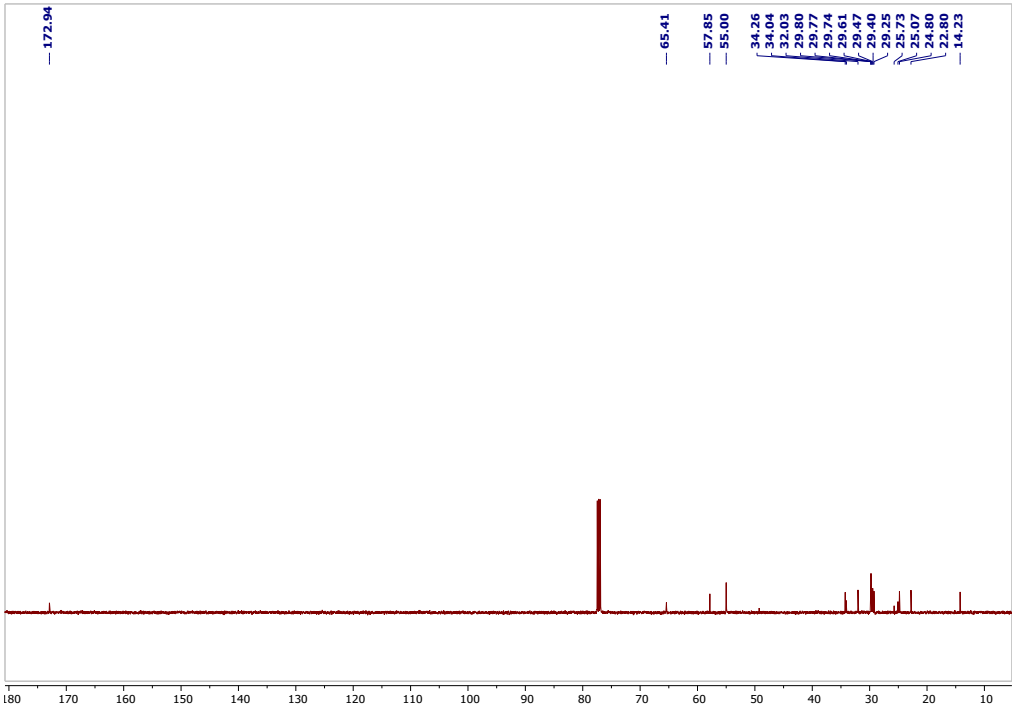

Figure S11: ^{13}C-NMR of OPC

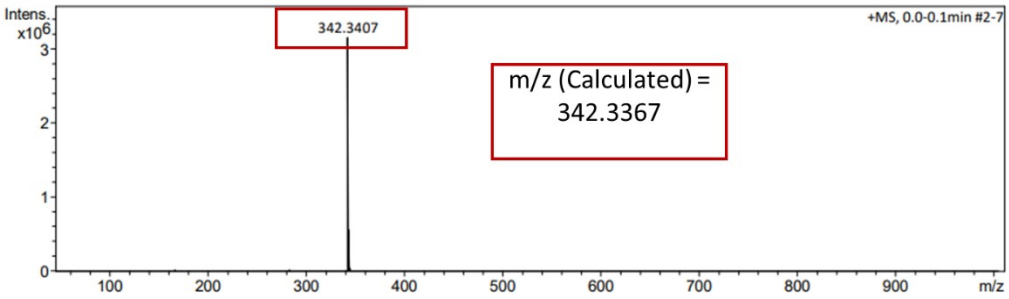

Figure S12: HRMS of chemically synthesized OPC.

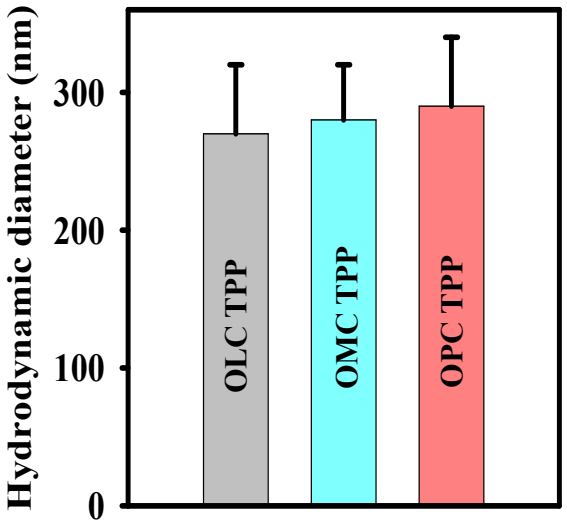

Figure S13: Average hydrodynamic diameter of OLC-TPP, OMC-TPP, and OPC-TPP aggregates from DLS experiments. Measurements were performed at least three times, and the average and standard deviation were plotted.

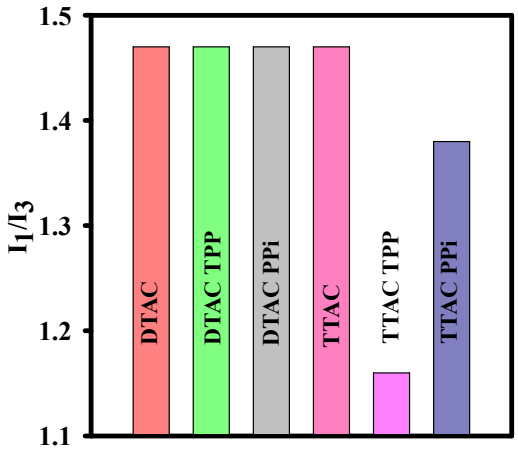

Figure S14: I_1/I_3 measurement of pyrene for different templated assemblies.

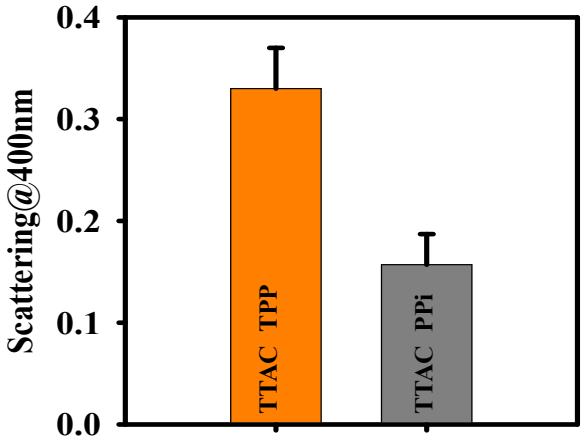

Figure S15: Scattering of TTAC-TPP, and TTAC-PPi templated assemblies.

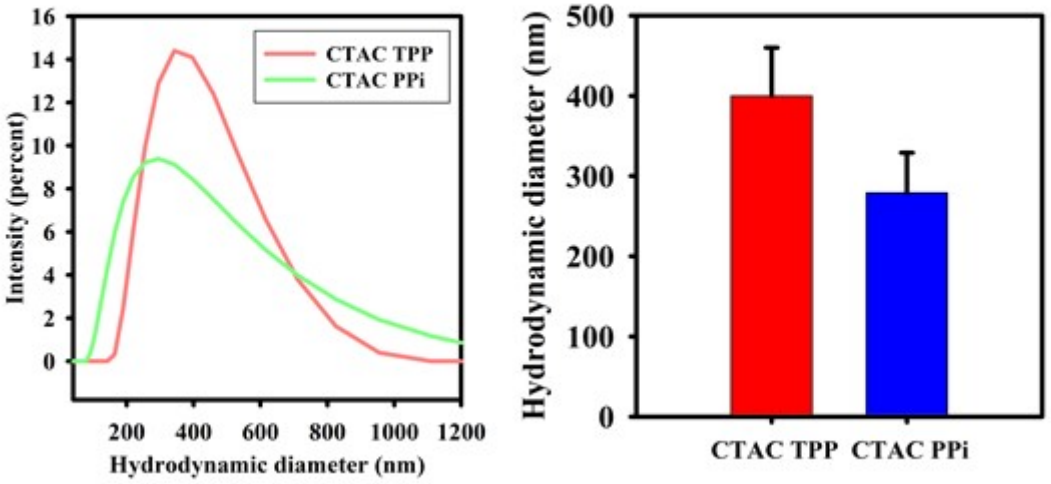

Figure S16: Average hydrodynamic diameter of **CTAC-TPP, and CTAC-PPi** aggregates from DLS experiments.

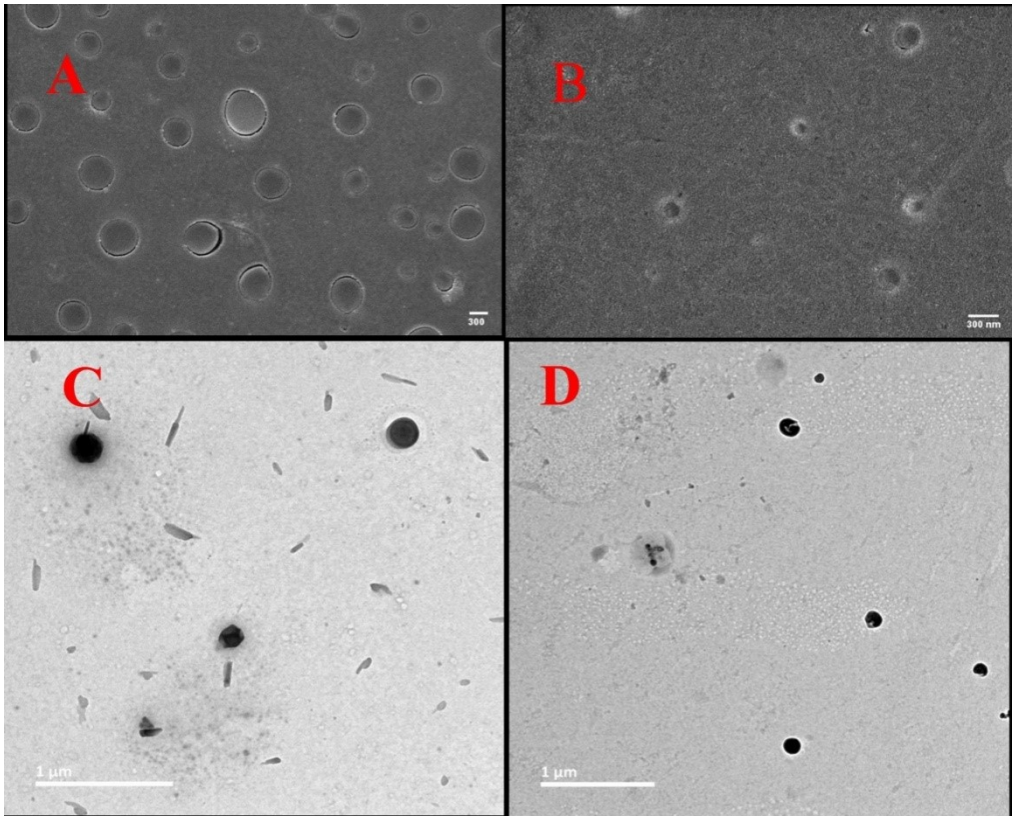

Figure S17: SEM images of CTAC-TPP (A) and CTAC-PPi (B), respectively. The scale bar is 300 nm in each case. TEM images of CTAC-TPP (C) and CTAC-PPi (D), respectively. The scale bar is 1000 nm in each case.

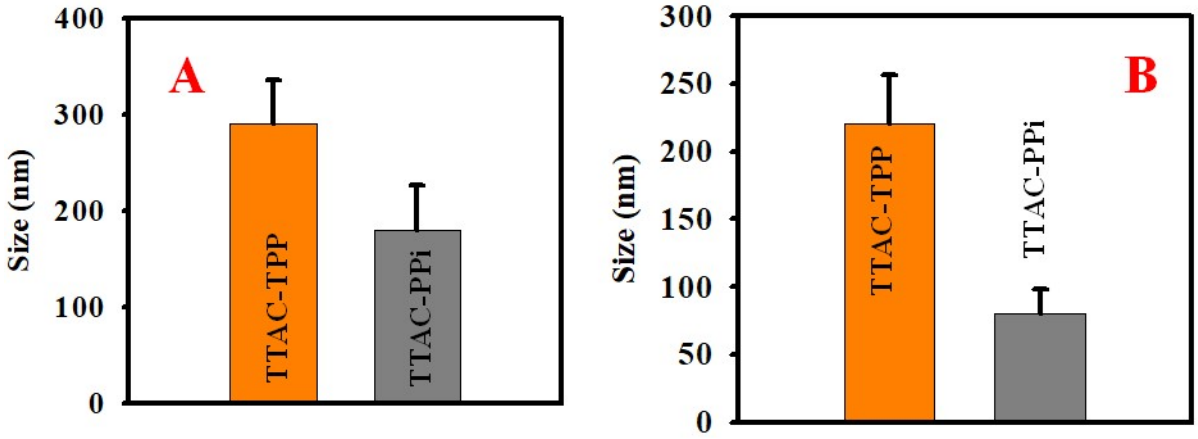

Figure S18: (A) The average size (nm) of the templated assembly of TTAC-TPP and TTAC-PPi was calculated from the SEM images, and (B) the average size (nm) of the templated assembly was calculated from the TEM images. Approximately 25 images were used for each case to calculate the standard deviation.

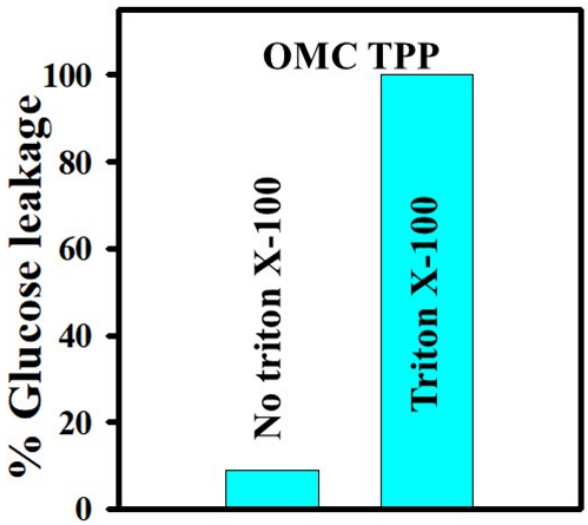

Figure S19. Glucose encapsulation of OMC-TPP vesicles and its leakage upon treatment with triton X-100.

Critical micelle concentration (CMC) and critical vesicle concentration (CVC) measurements

The CMC of TTAC was determined by fluorescence spectroscopic measurements using pyrene as a probe (λ_{ex}= 335 nm) in 10 mM tris-HCl, pH 7.0. The pyrene emission was recorded within a range from 350-550 nm. From that, I_1/I_3 (characteristic first and third emission peak of pyrene) were calculated and plotted against TTAC (mM) to get the CMC. The CMC was found

to be ~ 3.0 mM. Similar experiments were performed in the presence of TPP (TTAC-TPP), and PPi (TTAC-PPi) to determine the CVC in 10mM tris pH 7.0 buffer.

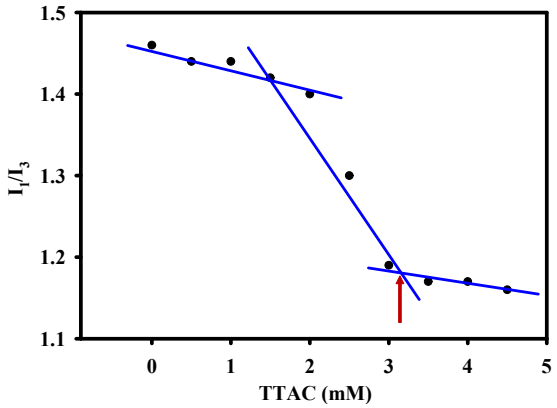

Figure S20: Determination of CMC of TTAC using pyrene.

Merocyanine 540 assay for CMC measurement

Merocyanine 540 assay is one of the convenient methods to calculate the critical micelle concentration and critical vesicle concentration (CVC). 1 mg / mL stock solution of merocyanine 540 was prepared in 50% ethanol. To get the CMC of TTAC, different concentrations of TTAC were prepared (1-6 mM overall concentration) at pH 7.0 tris-HCl buffer. In a 96 well-plate, 200 µL of TTAC was taken, and 0.75 µL of merocyanine 540 was added in each. The absorbance was recorded for each well from 400-650 nm range. The appearance of 570 nm peak indicates the aggregate formation.

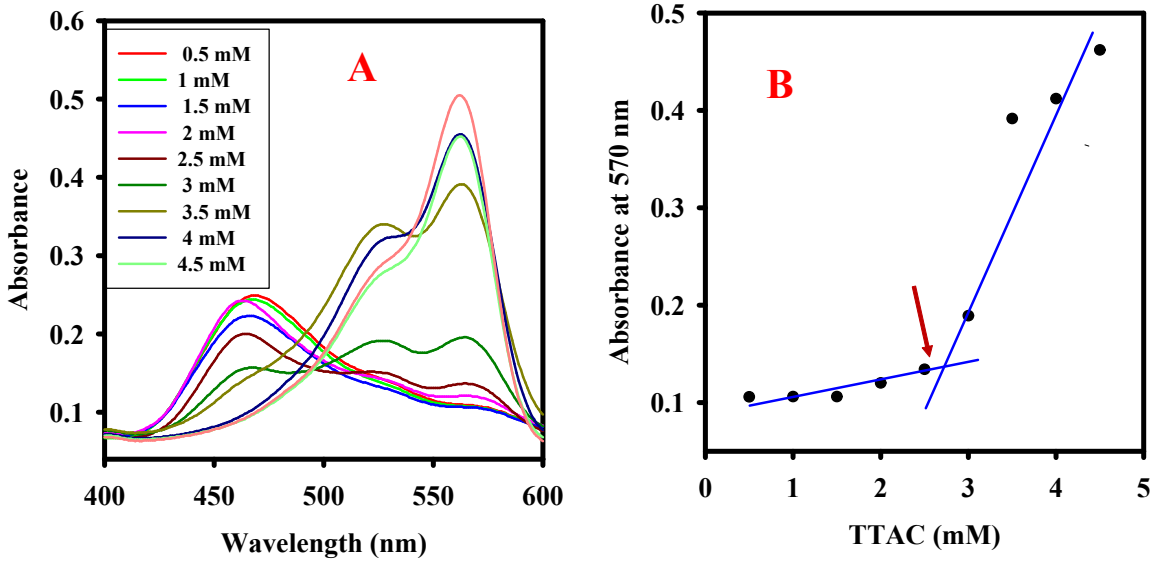

Figure S21: Determination of CMC using merocyanine 540 of TTAC. (A) The stacked absorption spectra of merocyanine 540 at increasing concentration of TTAC; (B) the absorbance at 570 nm was plotted against the concentration of TTAC. The inflection point indicated the CMC, which is around 3.0 mM.

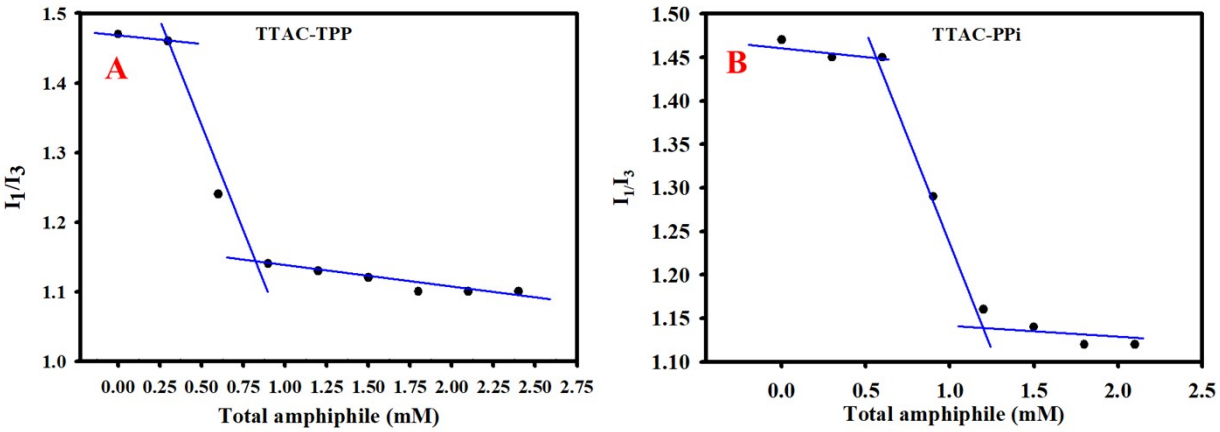

Figure S22: Determination of CVC of TTAC-TPP (A) and TTAC-PPi (B) using pyrene.

Merocyanine 540 assay for CVC measurement of TTAC-TPP

We performed the merocyanine 540 assays to get the CVC of TTAC-TPP in a similar way. Different concentrations of TTAC-TPP were prepared at pH 7.0 tris-HCl buffer. In a 96 well-plate 200 µL of TTAC-TPP (0.112-2 mM) was taken, and 0.75 µL of merocyanine 540 was added in each. The absorbance was recorded for each well from 400-650 nm range. The appearance of 570 nm peak indicates the aggregation. We have subtracted the scattering from the vesicular system before processing the merocyanine 540 absorbance.

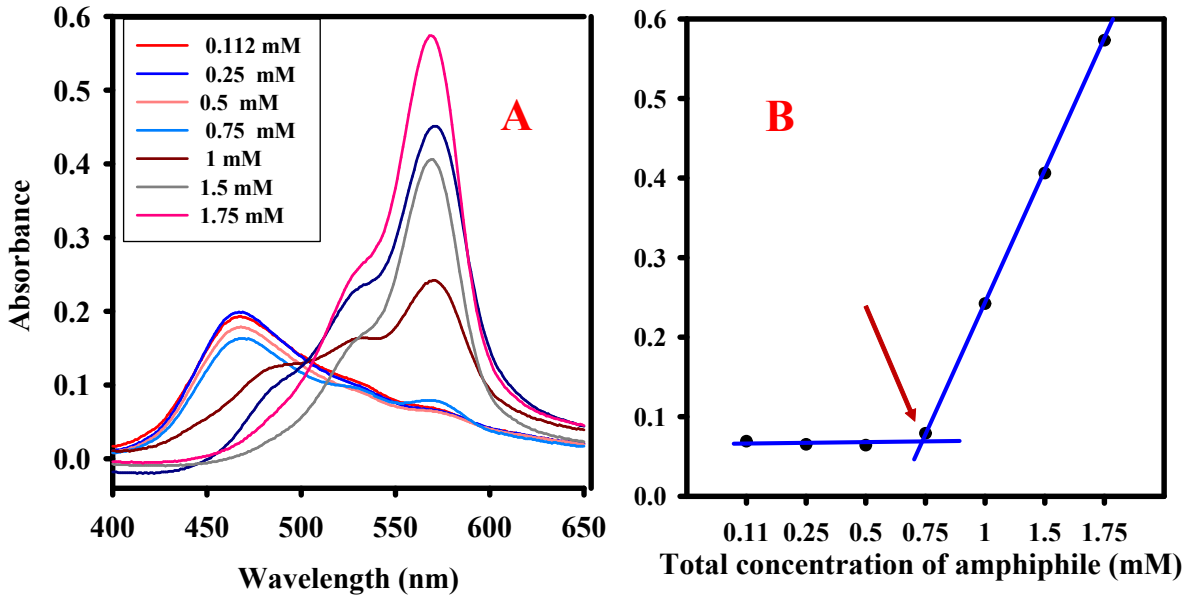

Figure S23: Determination of CVC using merocyanine 540 for TTAC-TPP. (A) The stacked absorption spectra of merocyanine 540 at increasing concentration of TTAC-TPP; (B) the absorbance at 570 nm was plotted against the total concentration of amphiphiles. The inflection point indicated the CVC which is around 0.75 mM (TTAC-TPP).

Merocyanine 540 assay for CVC measurement of TTAC-PPi

Like TTAC-TPP, we measured the CVC of TTAC-PPi, and it was ~ 1.25 mM.

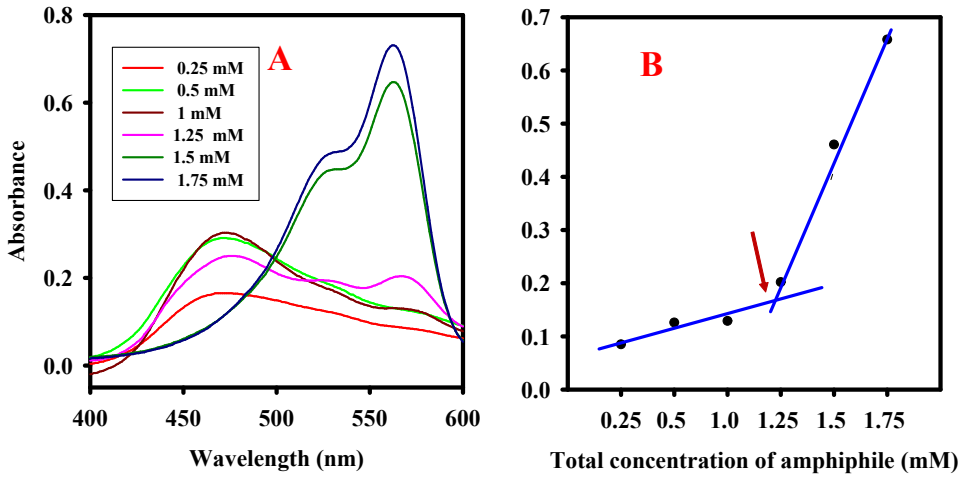

Figure S24: Determination of CVC using merocyanine 540 for TTAC-PPi. (A) The stacked absorption spectra of merocyanine 540 at increasing concentration of TTAC-PPi; (B) the absorbance at 570 nm was plotted against the total concentration of amphiphile. The inflection point indicated the CVC which is around 1.25 mM of TTAC-PPi.

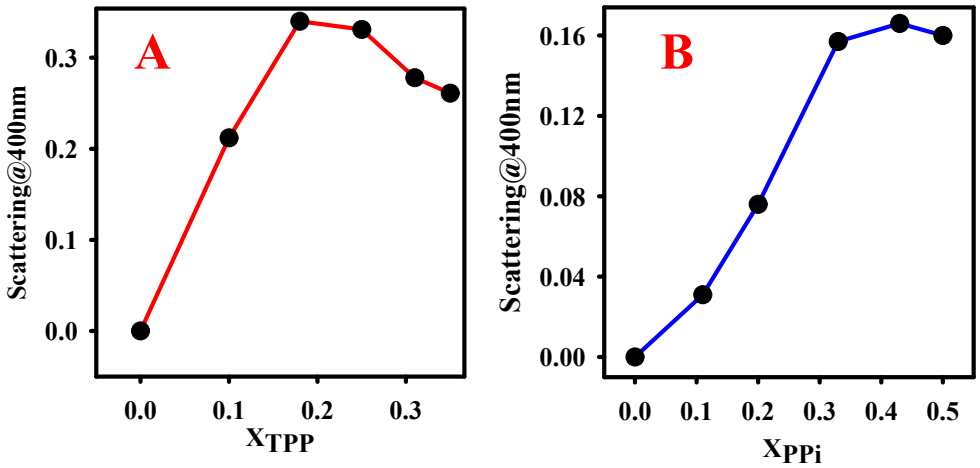

Figure S25. Turbidity measurements at 400 nm with different mixtures of (A) TPP-TTAC and (B) PPi-TTAC.

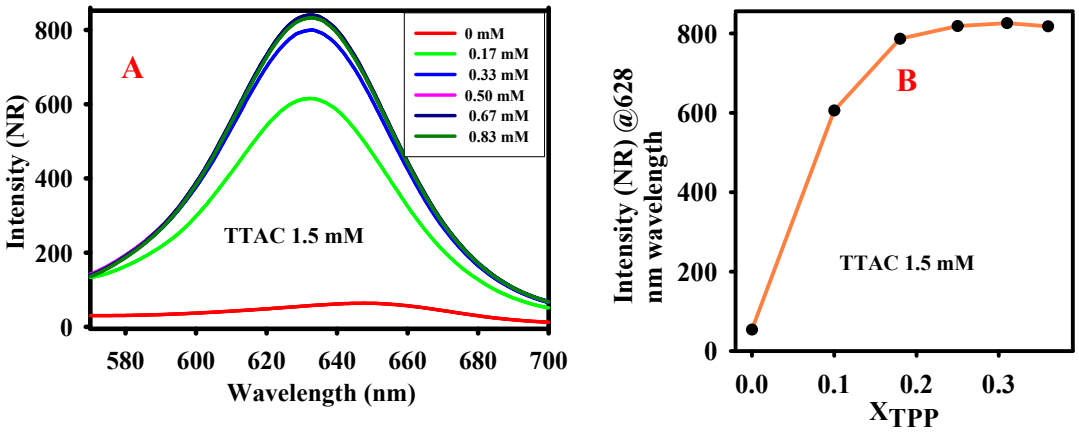

Figure S26: (A) Nile Red fluorescence increases with the gradual addition of TPP in 1.5 mM TTAC solution. (B) The plot of the fluorescence intensity of Nile Red *vs* different concentrations of TPP.

Powder X-ray diffraction (PXRD) studies: TTAC-TPP solution was prepared by mixing the appropriate amount of TTAC and TPP (3: 1) in water. The sample was lyophilized and the PXRD measurements were performed with a Rigaku (mini flex II, Japan) powder X-ray diffractometer having Cu Kα = 1.540 59 Å radiation. The dried samples were mounted on glass slides for diffraction. The scanning window was fixed up from 0-40°. PXRD of TTAC and TPP were also recorded to match the new peaks that appeared in the TTAC-TPP assembly.

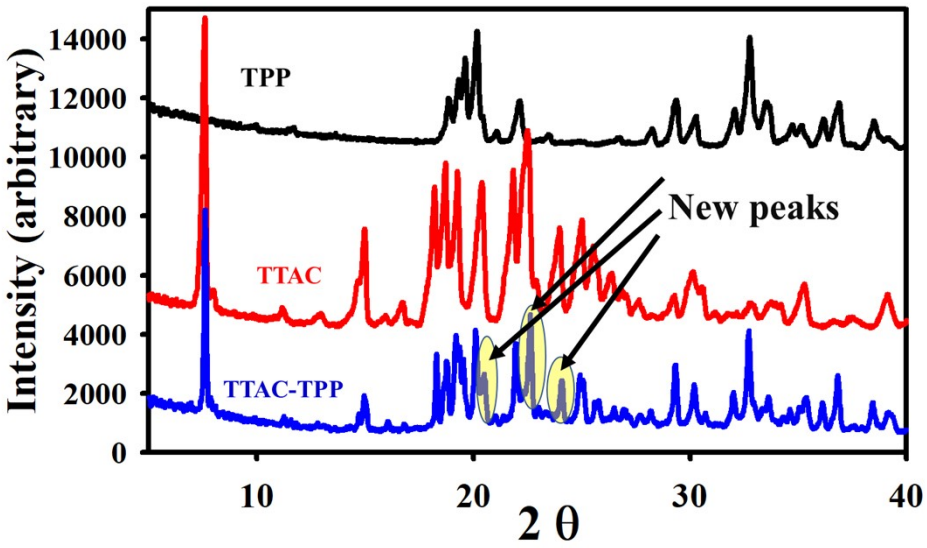

Figure S27: PXRD pattern of TTAC-TPP, TTAC, and TPP systems.

Table S1: Thermodynamic parameters from ITC experiment. Experiments were performed at 25 °C with 0.5 mM TTAC in the cell and 2.0 mM TPP (2.5 mM PPi) in the syringe. The low TTAC concentration was chosen to avoid further aggregation of 3: 1 or 2: 1 complex.

Parameters	**TTAC-TPP**	**TTAC-PPi**
N (Sites)	0.32 ± 0.06	0.51 ± 0.02
K_d (M)	13.0 ± 2.1 x 10^{-6}	22.1 ± 6.5 x 10^{-6}
ΔH (kcal /mol)	3.3 ± 0.2	2.7 ± 0.3
ΔG (kcal/mol)	-6.6	-6.3
-TΔS (kcal/mol)	-9.9	-9.0

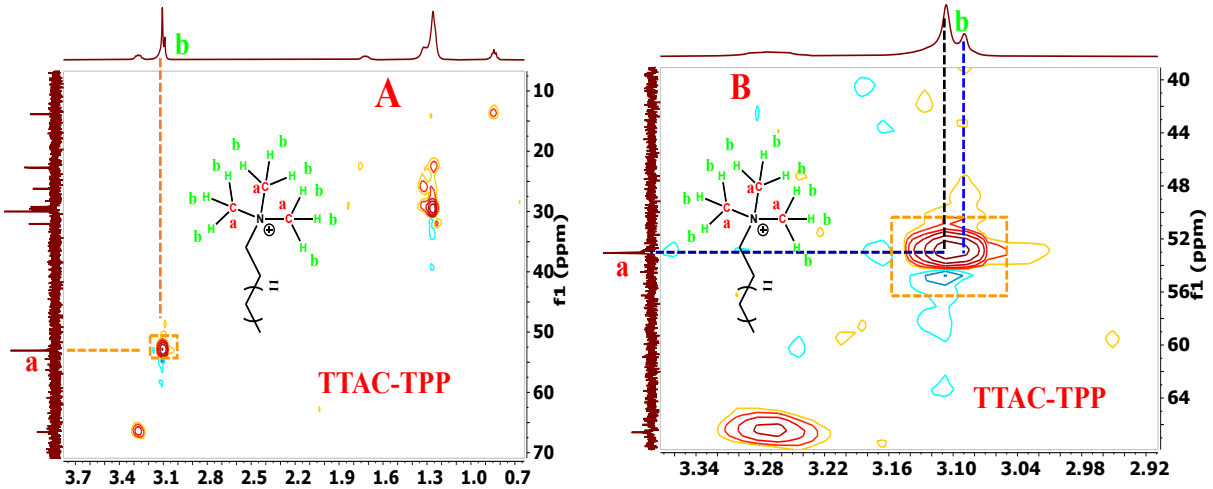

Figure S28: HSQC spectrum of TTAC-TPP. (A) full spectrum of TTAC-TPP and (B) zoomed spectrum at ~ 2.90-3.38 ppm. The spectrum was recorded in Bruker Avance 500 MHz spectrometer. 20 mM TTAC and 6.67 mM TPP were dissolved in D_2O to record the TTAC-TPP spectrum.

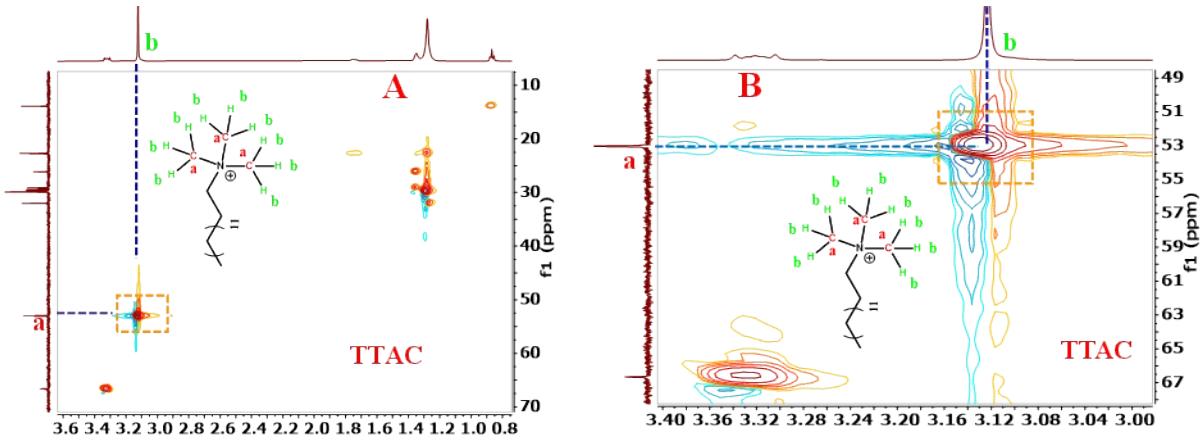

Figure S29: HSQC spectrum of TTAC. (A) full spectrum of TTAC and (B) zoomed spectrum. The spectrum was recorded in Bruker Avance 500 MHz spectrometer. 20 mM TTAC was dissolved in D_2O to record the TTAC spectrum.

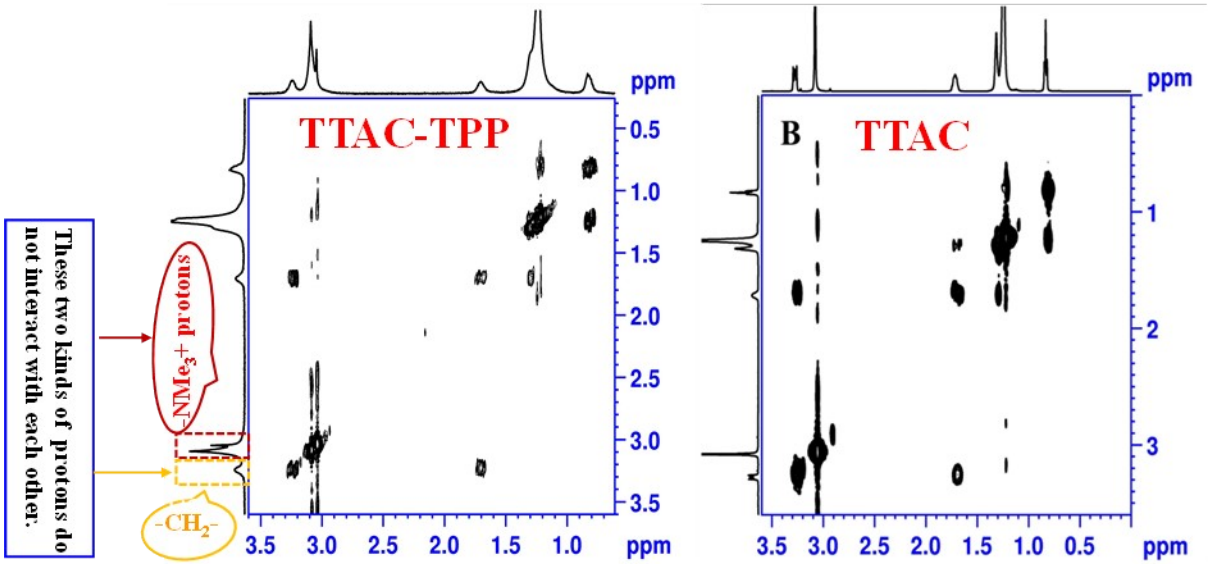

Figure S30: (A). COSY spectrum of TTAC-TPP. Protons of $-N^+Me_3$ do not interact with methylene protons, $-CH_2-$. (B) COSY spectrum of TTAC. The spectra were recorded in Bruker Avance 500 MHz spectrometer.

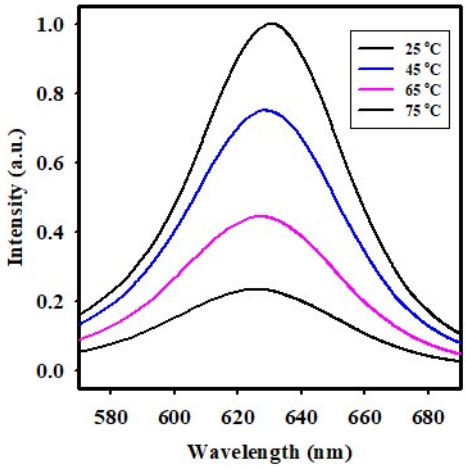

Figure S31: (A) Temperature-dependent Nile red fluorescence of TTAC-TPP. The intensity of Nile Red decreases with the elevation of temperature. The NR fluorescence intensity rapidly decreases above 45 ^{o}C. The decrease in fluorescence may suggest the modulation of the phase behavior at high temperatures and the formation of other assemblies. The partial hydrolysis of TPP at high temperatures could also lead to the above observations. We have shown that the NR fluorescence intensity of TTAC-PPi assembly was much lower than TTAC-TPP (Figure 2C).